Saudi Journal of Biological Sciences 29 (2022) 680–688

Contents lists available at ScienceDirect

Saudi Journal of Biological Sciences

journal homepage: www.sciencedirect.com

Original article

Phytosynthesis of silver nanoparticles from *Jatropha integerrima* Jacq. flower extract and their possible applications as antibacterial and antioxidant agent

Gunasekaran Suriyakala [a], Sivaji Sathiyaraj [a], Sandhanasamy Devanesan [b], Mohamad S. AlSalhi [b], Aruliah Rajasekar [c], Murali Kannan Maruthamuthu [d], Ranganathan Babujanarthanam [a,*]

[a] Nano and Energy Bioscience Laboratory, Department of Biotechnology, Thiruvalluvar University, Serkkadu, Vellore 632115, Tamil Nadu, India
[b] Department of Physics and Astronomy, College of Science, King Saud University, P.O. Box - 2455, Riyadh 11451, Saudi Arabia
[c] Environmental Molecular Microbiology Research Laboratory, Department of Biotechnology, Thiruvalluvar University, Serkkadu, Vellore, Tamilnadu 632115, India
[d] Department of Biotechnology & Bioengineering, Purdue University, 610 Purdue Mall, West Lafayette, IN 47907, United States

ARTICLE INFO

Article history:
Received 14 September 2021
Revised 3 December 2021
Accepted 4 December 2021
Available online 10 December 2021

Keywords:
Jatropha integerrima Jacq.
Silver nanoparticles
X-ray diffraction
E. coli
Superoxide

ABSTRACT

Jatropha integerrima Jacq. flower extract was used for the synthesis of silver nanoparticles in the current study. Various spectroscopic analyses were used to characterize the synthesized nanoparticles (JIF-AgNPs). The antibacterial efficacy of JIF-AgNPs was studied by well diffusion and microdilution techniques. In addition, the impact of JIF-AgNPs on free radicals was evaluated. On the ultraviolet–visible spectrum, the nanoparticles exhibit the highest absorbance at 422 nm. Based on the Fourier transform infrared spectrum, phenols and amino acids were involved in capping the JIF-AgNPs. Crystalline sphere-shaped nanoparticles with an average size of 50.07 nm and zeta potential of −19.0 mV were confirmed by X-ray diffraction, transmission electron microscopy, and dynamic light scattering analysis respectively. The JIF-AgNPs exhibit the highest and lowest growth inhibitory activity towards *E. coli* and *B. subtilis*. The minimal inhibitory concentration of JIF-AgNPs against *E. coli, K. pneumoniae, S. aureus*, and *B. subtilis* were 2.5, 5.0, 5.0, and 7.5 μg/mL, respectively. The JIF-AgNPs exhibited significant radical scavenging activities against DPPH (IC_{50}-32.5 ± 0.06 μg/mL), hydroxyl (IC_{50}-25 ± 0.09 μg/mL), Superoxide (IC_{50}-42.5 ± 0.13 μg/mL), and ABTs (IC_{50}-33.5 ± 0.15 μg/mL). Thus, synthesized nanoparticles were a good alternative to develop an antibacterial and antioxidant agent.

1. Introduction

The value of nanotechnology in the field of therapeutic medicine has expanded in recent days due to its wide variety of applications, cost-effective and eco-friendly approach for the preparation of novel drug materials (Kalaimurugan et al., 2019). Nanoparticles (NPs) with a size of 1–100 nm are considered essential building blocks in nanotechnology. Metals like gold, silver, copper, and zinc have sparked interest in the production of NPs due to their superior magnetic, electrical, medicinal, and optical capabilities. Silver nanoparticles (AgNPs) are familiar among different nanoparticles for their antibacterial, antioxidant, and cytotoxic properties (Das et al., 2019). Silver nanoparticles are the most often employed nanosized particles in various nanotechnology disciplines, particularly in biomedical applications (Elisabeta Barbinta-Patrascu et al., 2020).

Antimicrobial resistance is one of the most pressing issues of our time resulting from the inappropriate usage of antibiotics (Mboya et al., 2018). Solving this challenge will require a multidisciplinary strategy, including developing novel antimicrobial drugs (Talapko et al., 2020). Although silver's antibacterial action has been known since ancient times, many scientists are currently reinvestigating it, and the medicinal use of silver is on the rise (Sim et al., 2018). Silver nanoparticles exhibit exceptional antibacterial action even at low concentrations, so their utilization has steadily increased in recent decades (Yin et al., 2020). Metal nanoparticles, particularly silver nanoparticles are characterized

* Corresponding author.
E-mail address: babukmg@gmail.com (R. Babujanarthanam).
Peer review under responsibility of King Saud University.

Production and hosting by Elsevier

https://doi.org/10.1016/j.sjbs.2021.12.007
1319-562X/

by minimal toxicity towards human and great bactericidal potential (Hamouda et al., 2019). But the role of AgNPs on human cells is unknown when their antibacterial capability is considered in the context of human use. For instance, silver nanoparticles were less toxic to eukaryotic cells, combined with their antibacterial capability, could be particularly valuable in endodontic treatment when bacteria in the root canal system must be eliminated (Skóra et al., 2021). Silver NPs are also employed as antiseptic and disinfection agent because of their potential antibacterial property (Das et al., 2019).

Free radicals, which contribute to oxidative stress, cause the majority of oxidative illnesses (Inbathamizh et al., 2013). Free radicals majorly attack macromolecules such as proteins, lipids and nucleic acids which result in cell damage and homeostatic disruption (Lobo et al., 2010). Oxidative stress and free radical's damages were controlled by antioxidants. When oxidative stress and antioxidants are out of balance, diseases like aging, cancer, cardiovascular, autoimmune disorders, and neurological diseases can develop (Al-Rimawi et al., 2016). It is critical to synthesize chemical and naturally occurring antioxidants to minimize oxidative stress and its detrimental consequences. Many research publications have documented the ability of AgNPs to operate as an antioxidant by lowering the production of reactive oxygen species (ROS) and scavenging free radicals (Chokshi et al., 2016; Kiran et al., 2020; Zahoor et al., 2021).

Several methods were used to synthesize NPs; among them, biological method was less toxic and environmentally beneficial (Sathiyaraj et al., 2021). In the production of NPs, organic molecules act as a capping agent to aid in the stabilization of the NPs. Plant extracts are preferred over other biological approaches because they are readily available and contain various phytochemicals and metabolites that help reduce silver ions and speed up synthesis (Plackal Adimuriyil George et al., 2018). *Jatropha integerrima* Jacq. is a drought-tolerant perennial shrub that belongs to the family Euphorbiaceae. Various parts of *Jatropha integerrima* Jacq. has been employed as a purgative, styptic, and emetic in treating herpes, rheumatism, tumors, toothaches, warts, pruritis, eczema, scabies, and ringworm for centuries (Kolawole et al., 2017; Kuspradini et al., 2016). The leaves and seeds of the plant have antibacterial activity, while the branches have been proven to have cholinesterase activity, and the latex has anti-cancer activity (Ali et al., 2017; Eshilokun et al., 2019; Horsten et al., 1996; Sharma and Singh, 2012). Among 51 edible and wildflowers from China, the flower of *Jatropha integerrima* Jacq. exhibited the highest antioxidant capacity (Fu et al., 2010), implying that the flowers of *Jatropha integerrima* Jacq. could be a significant source of natural antioxidants. Proteins, phenols, steroids, flavonoids, and alkaloids, among other natural metabolites found in *Jatropha integerrima* Jacq., can operate as reducing agents and have favorable biological effects. As a result, NPs synthesized from *Jatropha integerrima* Jacq. could be used to develop a promising antibacterial and antioxidant agent with low cytotoxicity that could be used to combat major infectious illnesses. Considering the benefits of the plant, the present research was aimed to synthesis AgNPs using *Jatropha integerrima* Jacq. flower extract and synthesized silver nanoparticles (JIF-AgNPs) were then tested for antibacterial and free radical scavenging activities using appropriate techniques.

2. Materials and methods

2.1. Preparation of aqueous extract of plant material

Fresh plant material was collected from Thiruvalluvar University campus, Tamil Nadu, India and authenticated as *Jatropha integerrima* Jacq. by Dr. Jayaraman, plant anatomy research centre, Chennai, Tamil Nadu, India. The *Jatropha integerrima* Jacq. flower was cleansed then mashed with a homogenizer and shifted to a 250 mL container containing 100 mL of double-distilled water. It was thoroughly stirred for 10–15 min with a magnetic stirrer to make an aqueous flower extract. After that, aqueous flower extract was filtered and kept for future use.

2.2. Phytochemical analysis

Phytochemical screening was carried out to identify alkaloids, anthocyanin, anthraquinones, carbohydrates, coumarin, diterpene, flavanoid, glycosides, phenol, phlobatanin, protein, saponins, tannins, and terpenoids in the Jatropha integerrima Jacq. aqueous flower extract. These tests were done following the standard procedures (Oluwasogo Dada et al., 2019; Senguttuvan et al., 2014).

2.3. Synthesis of silver nanoparticles

Ten mL of flower extract was blended with 90 mL of 1 mM $AgNO_3$ to synthesis AgNPs, and the color shift was observed. The AgNPs were then spun at 15,000 rpm for 5–10 min at 4 °C, and the obtained pellet was suspended in double distilled water, dried, and kept at ambient temperature for future use.

2.4. Characterization techniques

The most basic and most easy technique for confirming the synthesis of nanoparticles is UV–Vis spectroscopy technique. The absorbance spectra of the colloidal sample were acquired in the 350–800 nm range using a UV–Vis spectrometer (UV) Shimadzu-UV 1800 and demineralized water as a blank. The functional groups in JIF-AgNPs were validated using Fourier Transform Infra-Red (FTIR) spectra from Perkin Elmer [Model RX1] with a wavelength range of 4000 to 650 cm^{-1}. The samples were combined with KBr powder and pelletized for FTIR analysis, and the spectrum data were recorded after drying. Bruker's D8-Advance used monochromatic Cu ka radiation (k = 1.5406 A) operated at 40 kV and 30 mA at a 2θ angle pattern to perform X-ray diffraction (XRD) examination. The result was compared to the International Centre for Diffraction Data (ICDD) collection to confirm the crystallinity of the JIF-AgNPs. The particle morphology and distribution were determined via the Transmission Electron Microscopy (TEM) examination. HITACHI H-800 TEM measurements were performed at 200 kV. A drop of the diluted JIF-AgNPs was kept on the copper grid, coated with carbon, and dried under light to create the TEM grid. EDX was used to check for the existence of metals in the sample. The size and stability of JIF-AgNPs were carried out in the Malvern instrument.

2.5. Antibacterial tests

The antibacterial activity of JIF-AgNPs was investigated using the well diffusion method (Suriyakala et al., 2021). The bacteria used in the experiment were *E. coli* (MTCC 448), *K. pneumoniae* (MTCC 109), *S. aureus* (ATCC 25923), and *B. subtilis* (MTCC 2394). 100 μL of fresh culture was dispersed on sterile petri plates containing Muller Hinton agar media. The wells were made in the petri plates using a sterile crock borer and filled with varied concentrations of JIF-AgNPs (10, 20, 30, and 40 μg/mL) and 10 μg/mL of control (ampicillin), following which the petri plates were kept overnight at ambient temperature. After incubation, a zone was formed around the wells by inhibiting the growth of organisms, and the zone was measured in mm and compared with control.

2.5.1. Minimal inhibitory concentration (MIC)

A microdilution approach was used to evaluate the MIC of JIF-AgNPs (Alsalhi et al., 2020). Two-fold dilutions of JIF-AgNPs in varied concentration (1.25 to 10 μg/mL) was added into Muller Hinton broth containing 1×10^8 bacterial suspension and kept at 37 °C for one day. The MIC was assessed by the turbidity of the sample to find the lowest dose of JIF-AgNPs that impedes 90% of bacterial growth. The experiment was triplicated to ensure the result for all the examined microorganisms.

2.6. Free radicals scavenging activity

Free radicals scavenging activity of JIF-AgNPs were studied at varied concentrations (10, 20, 30, 40, & 50 μg/mL). The free radicals scavenging activity of JIF-AgNPs against 2,2-diphenyl-1-picryl-hydrazyl-hydrate (DPPH) was calculated by the procedure suggested by Chen et al., (Chang et al., 2019). DPPH responds to an antioxidant compound by accepting an electron and gets lowered. The color transition from purple to yellow was read at 517 nm spectrophotometrically. The color transition depended on the quantity and quality of the sample used (NilamberLal Das et al., 2019). The hydroxyl (OH^-) scavenging was evaluated by the Ansar et al. (Ansar et al., 2020) process. OH^- radicals are formed by reducing hydrogen peroxide in the presence of JIF-AgNPs and vitamin C from transition metal ions. Superoxide (O_2^-) anion scavenging was analyzed by the experiment suggested by Gunaseelan (Gunaseelan et al., 2017). In a phenazine methosulphate (PMS)-NADH system, O_2^- radicals were produced by NADH oxidation and NBT reduction, which was observed to form a violet complex. The 2,2′-azino-bis(3-ethyl benzothiazoline-6-sulfonic acid (ABTs) scavenging was determined by the Kang and Kim method (Kang and Kim, 2019). ABTs were formed by the reaction between ABTs and potassium persulfate, which results in the generation of blue/green color chromophores. The addition of JIF-AgNPs rivals ABTs and decreases the color formation, and it was read spectrophotometrically. The percentage scavenging of free radicals was calculated by the formula followed.

$$Percent\ \ scavenging = \frac{A0 - A1}{A0} \times 100$$

Here, A0 = Control's absorbance and A1 = Sample's absorbance.

2.7. Statistical analysis

Results were expressed as mean ± standard error of data from three repeats and IBM SPSS statistics 25 software was used for statistical analysis.

3. Results

3.1. Phytochemical analysis

As stated in Table 1, the phytochemical components of *Jatropha integerrima* Jacq.'s aqueous flower extract were screened qualitatively. Anthocyanin, carbohydrate, coumarin, glycoside, phenol, protein, saponin, and tannin were present in the Jatropha integerrima Jacq. flower extract; while alkaloid, anthroquinone, diterpine, flavanoid, phlobatanin, and terpenoids were absent.

3.2. Synthesis and optical characterization of JIF-AgNPs

Aqueous flower extract of *Jatropha integerrima* Jacq. was used as reducing agents in the bio-depletion of silver ions into nanosized silver nanoparticles. A visible color shift was seen (pale pink to dark brown) and validated by UV–Vis spectral analysis. At the ideal condition, JIF-AgNPs exhibited a peak at 422 nm, confirming the formation of AgNPs by UV–Visible analysis (Fig. 1). Functional groups involved in the synthesis and capping process were studied by FTIR analysis. FTIR bands at 3136, 2117, 1897, 1612, 1349, 1004, and 758 cm^{-1} were found in the JIF-AgNPs (Fig. 2).

3.3. Structural characterization of JIF-AgNPs

The XRD was used to assess the crystallinity of the green synthesized NPs. Fig. 3 shows four notable diffraction peaks at 37.8°, 44.0°, 64.2°, and 77.2°, which correspond to the reflection of the 111, 200, 220, and 311 planes respectively (ICDD file No 04-0783).

According to TEM images, silver nanoparticles synthesized were widely dispersed and are predominantly spherical in shape (Fig. 4A). An average diameter of 29 nm and a size range of 17–45 nm was found in JIF-AgNPs (Fig. 4B). The results of SAED analysis revealed that the JIF-AgNPs contain fine crystalline NPs (Fig. 4C). The EDX was used to determine the elemental content of the AgNPs synthesized. Due to surface plasmon resonance, the EDX exhibit a significant peak at 3 keV (Fig. 4D), commonly seen in metallic silver nanocrystals. The EDX analysis confirmed the presence of some other elements along with silver (60.06%), they include carbon (18.10%), oxygen (16.65%), potassium (4.41%), and sodium (0.78%).

Using DLS, the particle size of JIF-AgNPs in an aqueous solution was determined. The size of JIF-AgNPs was 50.07 nm, according to the DLS analysis (Fig. 5A). Zeta potential analysis can be used to find out about the surface properties and stability of JIF-AgNPs. As shown in Fig. 5B, the zeta potential of JIF-AgNPs in our work was −19.0 mV.

3.4. Antibacterial activity

Green synthesized AgNPs were tested against various harmful bacteria, including *E. coli, K. pneumoniae, S. aureus,* and *B. subtilis*. On all four bacterial strains studied, AgNPs demonstrated considerable antibacterial activity (Fig. 6). Furthermore, when compared to gram-positive bacteria, AgNPs showed effective antibacterial activity against gram-negative bacteria. The highest and lowest zone of inhibition (ZOI) was found in *E. coli* (23.33 ± 0.58 mm) and *B. subtilis* (12.67 ± 0.33 mm) among the different bacteria tested (Table 2).

The antibacterial activity of JIF-AgNPs were also assessed by the MIC. The minimum concentration at which no apparent development of the test organism was detected was recorded as the MIC (Table 3). The MIC for *K. pneumoniae* and *S. aureus* was 5.0 μg/mL, while the MIC for *E. coli* and *B. subtilis* was 2.5 and 7.5 μg/mL respectively.

3.5. Free radicals scavenging activity

Free radicals cause many diseases, including Parkinson's disease, neurological disorders, mild cognitive dysfunction, and aging. The number of free radicals in the human body is decreased when necessary dietary antioxidants are consumed. Antioxidant consumption increases the quality of life by preventing degenerative diseases (Guntur et al., 2018). Here, antioxidant properties of JIF-AgNPs were tested against DPPH, hydroxyl, superoxide, and ABTs radicals and compared with vitamin C. Varied concentrations (10–50 μg/mL) of JIF-AgNPs showed 16–66% of DPPH radical scavenging, 13–73% of hydroxyl radical scavenging, 12–70% superoxide radical scavenging, and 28–78% of ABTs radical scavenging activities. While the vitamin C showed highest percent scavenging activity than JIF-AgNPs against DPPH (22–83%), hydroxyl (30–89%), superoxide (25–96%) and ABTs (27–89%) (Table 4). The inhibitory concentration (IC_{50}) of JIF-AgNPs against DPPH, hydroxyl, superoxide, and ABTs radicals were calculated as 32.5 ± 0.06, 32.5 ± 0.09,

Table 1
Phytochemical analysis of *Jatropha integerrima Jacq.* flower extract. "+" denotes the existence of the compounds; "-" indicates an absence of the compounds, "++" indicates the presence of a compound with a high concentration.

S.No	Phytochemicals	Test	Interference	Result
1.	Alkaloid	Hager's test	Formation of yellow precipitate	_
2.	Anthocyanin	Sodium hydroxide test	The appearance of pink to violet color	+
3.	Anthroquinone	Borntrager's test	The appearance of pink, violet, or red color	_
4.	Carbohydrate	Molisch's test	Formation of purple color	+
		Fehling's test	Formation of red color	+
5.	Coumarin	Sodium hydroxide test	The appearance of yellow color	+
6.	Diterpine	Copper acetate test	The appearance of emerald green	_
7.	Flavanoid	Alkaline reagent test	The appearance of colorless solution	_
8.	Glycoside	Sulphuric acid test	Formation of a reddish color.	++
9.	Phenol	Ferric chloride test	The appearance of green color	++
10.	Phlobatanin	Hydrochloric acid test	Formation of red precipitate	_
11.	Protein	Xanthoproteic test	The appearance of yellow color	++
		Biuret	The appearance of violet color	++
12.	Saponin	Foam test	Formation of stable foam	+
13.	Tannin	Braymer's test	The appearance of green color	+
14.	Terpenoids	Salkowski test	The appearance of deep red color	_

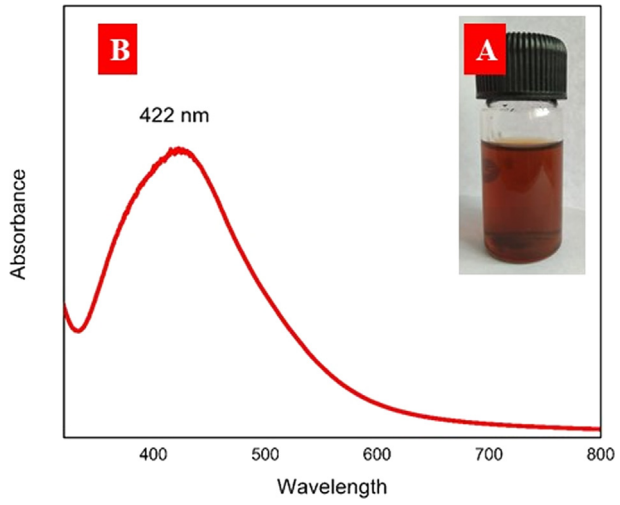

Fig. 1. A) Visual observation of JIF-AgNPs. B) UV–Visible spectrum of JIF-AgNPs.

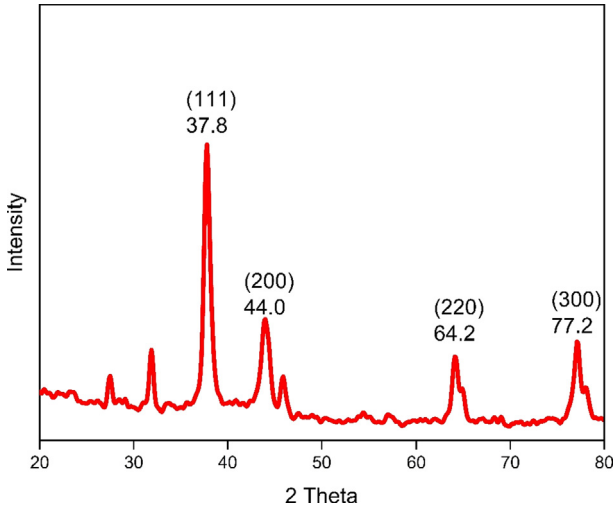

Fig. 3. Crystalline peaks of JIF-AgNPs.

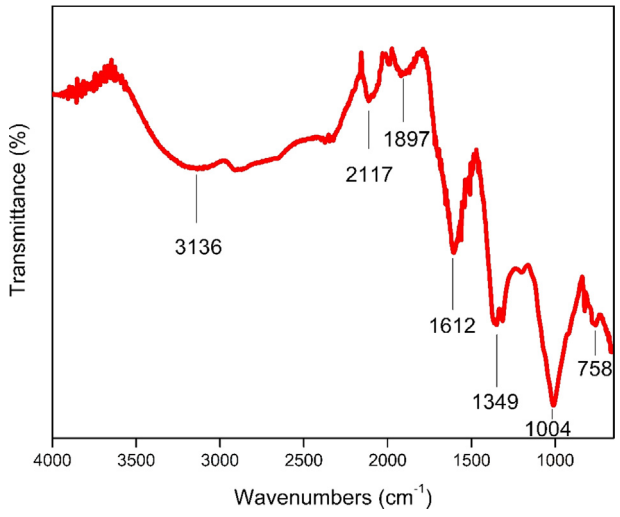

Fig. 2. FTIR spectrum of green synthesized silver nanoparticles.

42.5 ± 0.13, and 33.5 ± 0.15 μg/mL respectively. The IC_{50} value of vitamin C was calculated as 24 ± 0.02, 19.5 ± 0.04, 24.5 ± 0.03, and 22 ± 0.04 μg/mL for DPPH, hydroxyl, superoxide and ABTs radicals respectively (Table 4). These assays have proved the antioxidant potential of the JIF-AgNPs in comparison with the reference antioxidant, vitamin C.

4. Discussion

4.1. Characterization of JIF-AgNPs

Silver nanoparticles were synthesized by using *Jatropha integerrima* Jacq. flower extract as a reducing and capping agent. The existing phytochemicals of *Jatropha integerrima* Jacq. are involved in the capping and depletion of silver ions into silver nanoparticles (Hemlata et al., 2020). According to the literature, a 1:9 ratio (flower extract/$AgNO_3$) was necessary to generate particles with a spherical form (Salayová et al., 2021). JIF-AgNPs showed single peak at 422 nm in UV–Visible analysis. UV–Visible spectra can furnish useful details on particle morphology and distribution. The emergence of the peak in the UV–Vis spectra at a lower wavelength shows that the nanoparticles formed were small, whereas a lengthier wavelength indicates that the Ag-NPs formed were larger. According to Mie's hypothesis, spherical shaped nanoparticles produce a single SPR band in the UV–Vis spectrum (Abdulwahab et al., 2016).

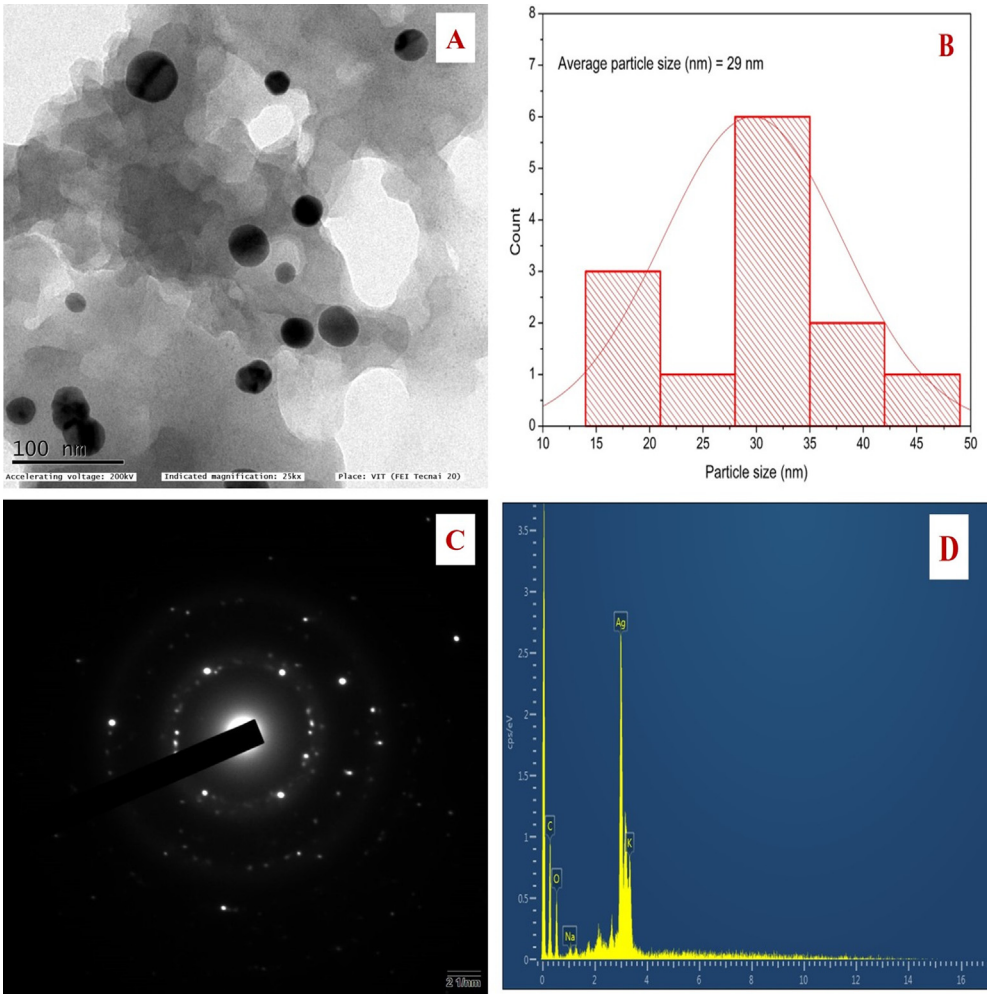

Fig. 4. A) Spherical shaped nanoparticles. B) Size distribution histogram C) SAED pattern of JIF-AgNPs. D) EDX spectrum.

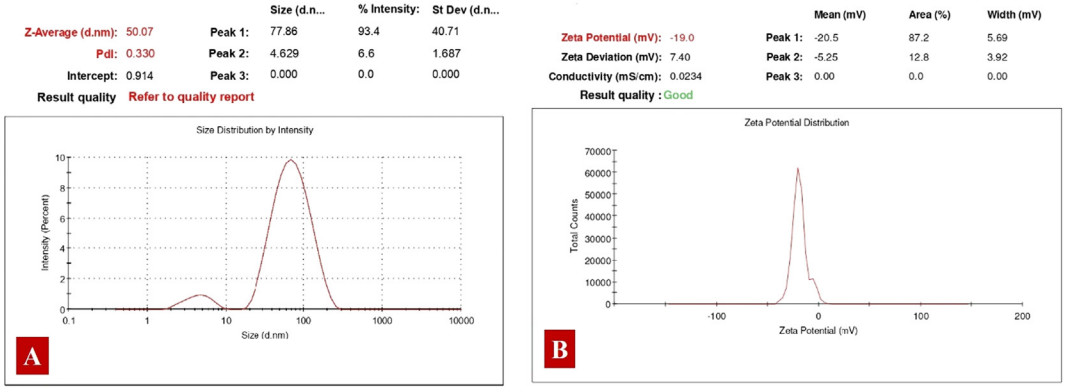

Fig. 5. A) Particle size of JIF-AgNPs. B) Stability of JIF-AgNPs.

FTIR analysis of JIF-AgNPs exhibits various peaks. The O-H strong stretching vibration of phenol and alcohol compounds correlates to the broad absorption FTIR peak at 3136 cm^{-1}. C=C from alkene or aromatic amine causes the weak band around 2117 cm^{-1} (Akintola et al., 2020). The (NH) C=O group was ascribed to the strong absorption peak at 1897 and 1612 cm^{-1} in the spectra (Devaraj et al., 2013; Imperio et al., 2013). O-H phenol has a prominent peak in the 1349 cm^{-1} region (Santhoshkumar et al., 2019). The C–H phenyl group was found at 758 cm^{-1} (Rivero-Montejo et al., 2021). These bands clearly define the presence of phenols and amino acids in flower extract act as a reducing and capping agent in the silver nanoparticle synthesis process.

The XRD result establishes the crystalline character of AgNPs (Dhand et al., 2016; rónavári et al., 2017). The four characteristic peaks at 37.8°, 44.0°, 64.2°, and 77.2°, represent the highly pure JIF-AgNPs (Anthony et al., 2014). In addition, some other peaks at

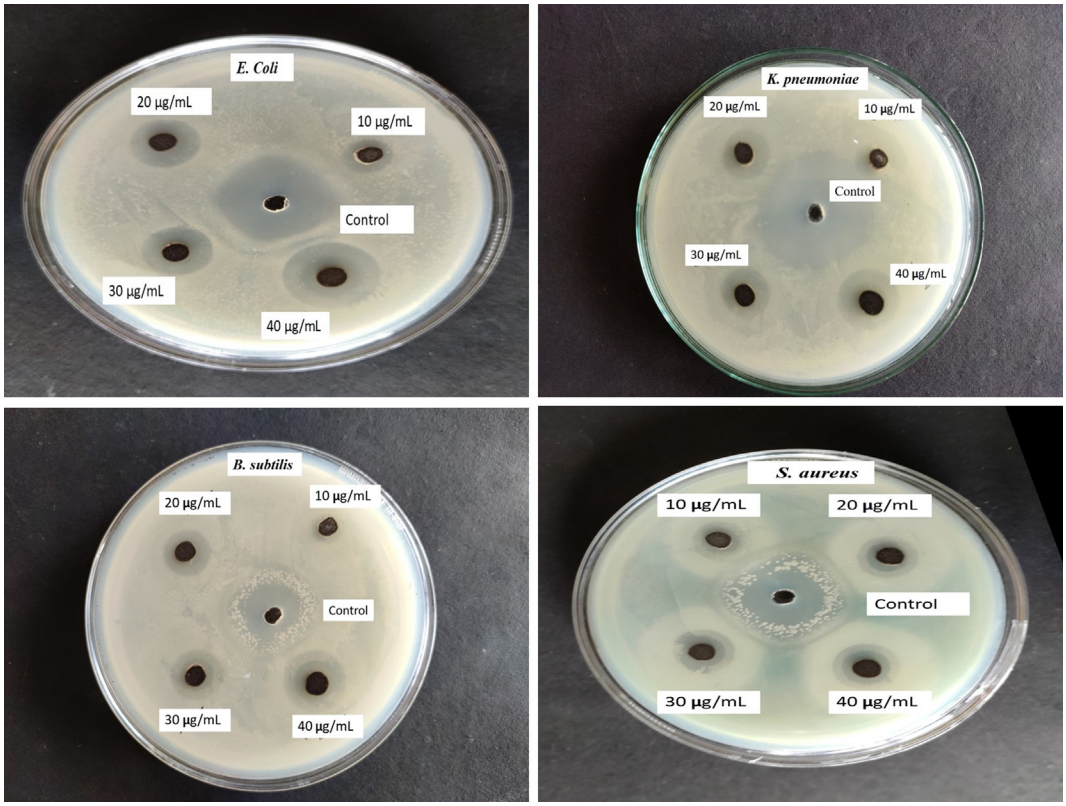

Fig. 6. Antibacterial activity of JIF-AgNPs against selected pathogenic bacteria at different concentrations.

Table 2
ZOI of JIF-AgNPs against selected pathogenic bacteria at various concentrations. Data were expressed as means ± standard error of data from three repeats.

Strain	ZOI (mm)				
	Control (10 µg/mL)	**10 µg/mL**	**20 µg/mL**	**30 µg/mL**	**40 µg/mL**
E. coli	29.33 ± 0.67	14.67 ± 0.33	17.66 ± 0.67	19.67 ± 0.33	23.33 ± 0.58
K. pneumoniae	31.67 ± 0.33	11.67 ± 0.33	13.33 ± 0.33	14 ± 0.58	18.33 ± 0.33
S. aureus	17.33 ± 0.33	9.67 ± 0.33	12 ± 0.58	13.33 ± 0.67	14.67 ± 0.33
B. subtilis	15.33 ± 0.33	7.33 ± 0.33	9.33 ± 0.33	11.67 ± 0.33	12.67 ± 0.33

Table 3
MIC of JIF-AgNPs against selected pathogenic strains.

S. No	Strain	MIC (µg/mL)
1	*E. coli*	**2.5**
2	*K. pneumoniae*	**5**
3	*S. aureus*	**5**
4	*B. subtilis*	**7.5**

27.5°, 31.9°, and 45.9° were also observed which was due to the presence of phytochemicals on the outer membrane of the NPs. The Braggs reflections occurring between 24.48° to 32.50° are frequently attributed to crystalline and amorphous organic phases (Gurunathan et al., 2014).

Spherical shaped, 17–45 nm-sized JIF-AgNPs were observed in TEM analysis. The corners of the generated silver nanoparticles were not brighter than the center in TEM micrographs, indicating the existence of biomolecules such as phenols and amino acids in *Jatropha integerrima* Jacq. flower that functions as a capping agent and inhibits aggregation. The stability of green synthesized NPs was based on the capping efficiency of the capping agent (Pugazhendhi et al., 2015).

The presence of randomly oriented particles with diameters in the nanometer range and their crystallinity were confirmed by SAED patterns in the form of diffraction rings. The diffraction rings indicate the crystalline nature of the JIF-AgNPs (Devanesan et al., 2021). Larger NPs contribute to brighter diffraction dots, while finer NPs contribute to lesser brightness diffraction dots. An additional factor contributing to the diffraction pattern's appearance is the thickness of the sample; in this case, the organic matrix is quite thick, which weakens the diffraction intensity from the smallest NPs (Salayová et al., 2021).

The elemental composition of JIF-AgNPs was observed by EDX analysis. Peaks for silver, carbon, oxygen, potassium, and sodium were observed. Peaks responsible for the other elements were due to the capping agents; this supports the presence of phytochemicals on the outer membrane of AgNP (Femi-Adepoju et al., 2019; Kambale et al., 2020).

By DLS analysis, particle size and zeta potential were calculated as 50.07 nm and −19.0 mV respectively. When compared to TEM analysis, DLS reported a bigger particle size. Because DLS primarily uses Rayleigh scattering, this occurrence was conceivable (Bernardo-Mazariegos et al., 2019). Similarly, DLS typically yielded greater results than TEM due to Brownian motion (Bragais and Labaclado, 2019; Krishnaraj et al., 2010). Because poly-dispersed samples tend to respond to bigger particles, these findings suggested that DLS measurement might not be accurate. Furthermore,

Table 4
Free radicals scavenging activity of vitamin C and JIF-AgNPs at varied concentrations against various free radicals. Results were expressed as mean ± standard error of data from three repeats. Different superscripts indicate the results were significant based on Duncan's method ($p < 0.05$).

Free Radical	Concentration	Vitamin C	JIF-AgNPs
DPPH	10 μg/mL	22.48 ± 0.03 ^{f}	16.60 ± 0.09 ^{f}
	20 μg/mL	42.62 ± 0.04 ^{d}	22.62 ± 0.10 ^{d}
	30 μg/mL	63.26 ± 0.04 ^{c}	48.62 ± 0.06 ^{c}
	40 μg/mL	76.48 ± 0.26 ^{b}	55.57 ± 0.07 ^{b}
	50 μg/mL	83.44 ± 0.01^{a}	66.73 ± 0.09 ^{a}
	IC_{50}	24 ± 0.02	32.5 ± 0.06
Hydroxyl	10 μg/mL	30.10 ± 0.05 ^{f}	13.25 ± 0.04 ^{f}
	20 μg/mL	50.13 ± 0.06 ^{d}	26.76 ± 0.07 ^{d}
	30 μg/mL	65.13 ± 0.08 ^{c}	47.57 ± 0.10 ^{c}
	40 μg/mL	84.28 ± 0.05 ^{ab}	60.51 ± 0.08 ^{b}
	50 μg/mL	89.62 ± 0.09 ^{a}	73.47 ± 0.03 ^{a}
	IC_{50}	19.5 ± 0.04	32.5 ± 0.09
Superoxide	10 μg/mL	25.60 ± 0.05 ^{f}	12.54 ± 0.20 ^{f}
	20 μg/mL	33.58 ± 0.06 ^{d}	25.42 ± 0.17 ^{d}
	30 μg/mL	59.16 ± 0.06 ^{c}	40.50 ± 0.25 ^{bc}
	40 μg/mL	84.79 ± 0.09 ^{b}	44.48 ± 0.18 ^{b}
	50 μg/mL	96.72 ± 0.11 ^{a}	70.53 ± 0.24 ^{a}
	IC_{50}	24.5 ± 0.03	42.5 ± 0.13
ABTs	10 μg/mL	27.70 ± 0.04 ^{f}	19.31 ± 0.15 ^{f}
	20 μg/mL	43.78 ± 0.10 ^{d}	33.70 ± 0.18 ^{d}
	30 μg/mL	61.44 ± 0.03 ^{c}	40.53 ± 0.21 ^{c}
	40 μg/mL	76.63 ± 0.08 ^{b}	72.55 ± 0.28 ^{b}
	50 μg/mL	89.51 ± 0.05 ^{a}	78.66 ± 0.14 ^{a}
	IC_{50}	22 ± 0.04	33.5 ± 0.15

as purification was not conducted during the synthesis, the presence of agglomerated phytochemicals in the solution revealed that it contained big particles (Bernardo-Mazariegos et al., 2019; Kouhbanani et al., 2019). The zeta potential value obtained for JIF-AgNPs is within the stable range, indicating that the nanoparticles are stable in an aqueous solution. The negative zeta potential nanoparticles were prevented from aggregation and stabilized by electrostatic repulsion (Paosen et al., 2017).

4.2. Antibacterial activity

The finding demonstrated that JIF-AgNPs have an antibacterial effect against all tested bacteria. The electrostatic attraction between the negatively charged cell membrane of the organism and the Ag^{+} ion can be explained as a plausible mechanism of the antibacterial activity. As a result, the Ag^{+} ion can be bound with a specific group of enzymes, namely thiol, destroying the capacity to replicate DNA and causing bacterial cell death (Li et al., 2016). According to Wan Mat Khalir et al., (Wan Mat Khalir et al., 2020), the plausible mechanisms might be substituted by the direct contact between JIF-AgNPs and the bacterial surface, which causes DNA replication to be disrupted and the production of ROS, and result in bacterial cell death (Devanesan et al., 2020; Devanesan and Alsalhi, 2021). In addition, AgNPs are more efficient against gram-negative bacteria than gram-positive bacteria. The discrepancies in results were due to structural variation between gram-positive and gram-negative bacteria (Grigor'Eva et al., 2013; Kawahara et al., 2000). In comparison to gram-negative bacteria, gram-positive bacteria have a thicker cell wall due to numerous layers of peptidoglycan (Thiel et al., 2007). So, it is difficult to enter into gram-positive bacteria than gram-negative bacteria (Erjaee et al., 2017). Earlier studies have shown that AgNPs were active against a wide range of pathogenic bacteria due to their effective antibacterial properties (Gandhi et al., 2021; Skóra et al., 2021; Urnukhsaikhan et al., 2021).

4.3. Free radicals scavenging activity

The DPPH assay is on the basis of the depletion of DPPH in methanol solution, where radical DPPH was changed to non-radical DPPHH by receiving a hydrogen molecule in the existence of a hydrogen–donating antioxidant. The color shift from purple to yellow was visually noticed and read spectrophotometrically at 517 nm. The scavenging action of varied doses of JIF-AgNPs (10–50 μg/mL) on the DPPH radical is demonstrated in this study. The mutagenic capability of free radicals owes a link between OH^{-} radicals and DNA, leads to DNA breakage and, hence, cause cancer (Khan et al., 2013). JIF-AgNPs remove OH^{-} radicals and prevent additional damages. Compared to typical antioxidants, AgNPs demonstrated significant hydroxyl radical scavenging activity and may be used as anticancer therapeutics by blocking the link between OH^{-} radicals and DNA (Rahman et al., 2015). Superoxide is essential in biology because it produces singlet oxygen and hydroxyl radicals. Overproduction of the superoxide anion radical causes redox imbalance, which has negative physiological implications. Superoxide anions are produced by a variety of biological processes and are extremely hazardous. The superoxide anion produced by the PMS/NADH decreases NBT in the PMS/NADH-NBT system (Basniwal et al., 2009). The decolorization of the ABTS radical cation, which was detected spectrophotometrically at 734 nm, was used to quantify the total antioxidant activity of JIF-AgNPs. The absorbance of the ABTS radicals was suppressed by interaction with JIF-AgNPs or vitamin C, and the data were represented as percentage inhibition of absorbance (Gangwar et al., 2014). The findings revealed that different concentrations of JIF-AgNPs exhibited varying degrees of radical scavenging capacity in a concentration-dependent manner.

5. Conclusion

The AgNPs were synthesized by using an aqueous flower extract of *Jatropha integerrima* Jacq. and the green synthesis process was known to be easy, eco-friendly, and cost-effective. Phytochemicals from the extract were involved for the synthesis of nanoparticles and various characterization techniques were used in this investigation to establish the successful formation of spherical shaped and crystalline AgNPs. Furthermore, JIF-AgNPs had good bactericidal effect against *E. coli*, *K. pneumoniae*, *S. aureus*, and *B. subtilis*. In addition, green synthesized AgNPs were effective scavengers of DPPH, hydroxyl, superoxide, and ABTS radicals, suggesting that they could be used as a drug to eliminate free radicals and prevent cellular damage.

Declaration of Competing Interest

The authors declare that they have no known competing financial interests or personal relationships that could have appeared to influence the work reported in this paper.

Acknowledgment

The authors acknowledge, Department of Biotechnology, Thiruvalluvar University, Serkkadu, Vellore, India. The authors extend their appreciation to the Researchers Supporting Project number (RSP-2021/398), King Saud University, Riyadh, Saudi Arabia.

References:

Abdulwahab, F., Henari, F.Z., Cassidy, S., Winser, K., 2016. Synthesis of Au, Ag, curcumin Au/Ag, and Au-Ag nanoparticles and their nonlinear refractive index properties. J. Nanomater. 2016, 1–7. https://doi.org/10.1155/2016/5356404.
Akintola, A.O., Kehinde, B.D., Ayoola, P.B., Adewoyin, A.G., Adedosu, O.T., Ajayi, J.F., Ogunsona, S.B., 2020. Antioxidant properties of silver nanoparticles

biosynthesized from methanolic leaf extract of Blighia sapida. IOP Conference Series: Mater. Sci. Eng. 805 (1), 012004. https://doi.org/10.1088/1757-899X/805/1/012004.
Ali, M., Sharma, S.K., Singh, H., Sultnaa, S., Mir, S.R., 2017. Phytochemical Investigation of the Roots of Jatropha Integerrima Jacq. J. Progressive Res. Chem. 4, 194–200.
Al-Rimawi, F., Rishmawi, S., Ariqat, S.H., Khalid, M.F., Warad, I., Salah, Z., 2016. Anticancer Activity, Antioxidant Activity, and Phenolic and Flavonoids Content of Wild Tragopogon porrifolius Plant Extracts. Evidence-based Complementary Alternative Med. 2016, 1–7. https://doi.org/10.1155/2016/9612490.
Alsalhi, M.S., Devanesan, S., Atif, M., Alqahtani, W.S., Nicoletti, M., del Serrone, P., 2020. Therapeutic potential assessment of green synthesized zinc oxide nanoparticles derived from fennel seeds extract. Int. J. Nanomed. https://doi.org/10.2147/IJN.S272734.
Ansar, S., Tabassum, H., M Aladwan, N.S., Naiman Ali, M., Almaarik, B., AlMahrouqi, S., Abudawood, M., Banu, N., Alsubki, R., 2020. Eco friendly silver nanoparticles synthesis by Brassica oleracea and its antibacterial, anticancer and antioxidant properties. https://doi.org/10.1038/s41598-020-74371-8.
Anthony, K.J.P., Murugan, M., Jeyaraj, M., Rathinam, N.K., Sangiliyandi, G., 2014. Synthesis of silver nanoparticles using pine mushroom extract: a potential antimicrobial agent against E. coli and B. subtilis. J. Ind. Eng. Chem. 20 (4), 2325–2331. https://doi.org/10.1016/j.jiec.2013.10.008.
Basniwal, P., Suthar, M., Rathore, G., Gupta, R., Kumar, V., 2009. In-vitro antioxidant activity of hot aqueous extract of Helicteres isora Linn. fruits.
Bernardo-Mazariegos, E., Valdez-Salas, B., González-Mendoza, D., Abdelmoteleb, A., Tzintzun Camacho, O., Ceceña Duran, C., Gutiérrez-Miceli, F., 2019. Silver nanoparticles from Justicia spicigera and their antimicrobial potentialities in the biocontrol of foodborne bacteria and phytopathogenic fungi. Rev. Argent. Microbiol. 51 (2), 103–109. https://doi.org/10.1016/j.ram.2018.05.002.
Bragais, E.K.B., Labaclado, L.M., 2019. Green Synthesis, Characterization and Antimicrobial Activity of Silver Nanoparticles Using Dudoa (Hydnocarpus alcalae C.DC.) Leaf Extract As a Reducing and Stabilizing Agent. Curr. Nanomater. 4 (2), 112–124. https://doi.org/10.2174/2405461504666190617100254.
Chang, C.-C., Chen, C.-P., Wu, T.-H., Yang, C.-H., Lin, C.-W., Chen, C.-Y., 2019. Gold nanoparticle-based colorimetric strategies for chemical and biological sensing applications. Nanomaterials 9 (6), 861. https://doi.org/10.3390/nano9060861.
Chokshi, K., Pancha, I., Ghosh, T., Paliwal, C., Maurya, R., Ghosh, A., Mishra, S., 2016. Green synthesis, characterization and antioxidant potential of silver nanoparticles biosynthesized from de-oiled biomass of thermotolerant oleaginous microalgae Acutodesmus dimorphus. RSC Adv. 6 (76), 72269–72274. https://doi.org/10.1039/C6RA15322D.
Das, G., Patra, J.K., Debnath, T., Ansari, A., Shin, H.S., 2019. Investigation of antioxidant, antibacterial, antidiabetic, and cytotoxicity potential of silver nanoparticles synthesized using the outer peel extract of Ananas comosus (L.). PLoS ONE 14. https://doi.org/10.1371/journal.pone.0220950.
Devanesan, S., Alsalhi, M.S., 2021. Green Synthesis of Silver Nanoparticles Using the Flower Extract of Abelmoschus esculentus for Cytotoxicity and Antimicrobial Studies. https://doi.org/10.2147/IJN.S307676.
Devanesan, S., Jayamala, M., AlSalhi, M.S., Umamaheshwari, S., Ranjitsingh, A.J.A., 2021. Antimicrobial and anticancer properties of Carica papaya leaves derived di-methyl flubendazole mediated silver nanoparticles. J. Infection Public Health 14 (5), 577–587. https://doi.org/10.1016/j.jiph.2021.02.004.
Devanesan, S., Ponmurugan, K., AlSalhi, M.S., Al-Dhabi, N.A., 2020. Cytotoxic and Antimicrobial Efficacy of Silver Nanoparticles Synthesized Using a Traditional Phytoproduct, Asafoetida Gum. Int. J. Nanomed. 15, 4351. https://doi.org/10.2147/IJN.S258319.
Devaraj, P., Kumari, P., Aarti, C., Renganathan, A., 2013. Synthesis and characterization of silver nanoparticles using cannonball leaves and their cytotoxic activity against MCF-7 cell line. J. Nanotechnol. 2013, 1–5. https://doi.org/10.1155/2013/598328.
Dhand, V., Soumya, L., Bharadwaj, S., Chakra, S., Bhatt, D., Sreedhar, B., 2016. Green synthesis of silver nanoparticles using Coffea arabica seed extract and its antibacterial activity. Mater. Sci. Eng., C 58, 36–43. https://doi.org/10.1016/j.msec.2015.08.018.
Elisabeta Barbinta-Patrascu, M., Ungureanu, C., Badea, N., Bacalum, M., Lazea-Stoyanova, A., Zgura, I., Negrila, C., Enculescu, M., Burnei, C., 2020. Novel ecogenic plasmonic biohybrids as multifunctional bioactive coatings. Coatings 10, 659. https://doi.org/10.3390/coatings10070659.
Erjaee, H., Rajaian, H., Nazifi, S., 2017. Synthesis and characterization of novel silver nanoparticles using Chamaemelum nobile extract for antibacterial application. Adv. Nat. Sci.: Nanosci. Nanotechnol. 8 (2), 025004. https://doi.org/10.1088/2043-6254/aa690b.
Eshilokun, A.O., Kasali, A.A., Ogunwande, I.A., Walker, T.M., Setzer, W.N., 2019. Chemical Composition and Antimicrobial Studies of the Essential Oils of Jatropha integerrima Jacq (Leaf and Seeds): https://doi.org/10.1177/1934578X0700200813 2, 853–855. https://doi.org/10.1177/1934578X0700200813.
Femi-Adepoju, A.G., Dada, A.O., Otun, K.O., Adepoju, A.O., Fatoba, O.P., 2019. Green synthesis of silver nanoparticles using terrestrial fern (Gleichenia Pectinata (Willd.) C. Presl.): characterization and antimicrobial studies. Heliyon 5 (4), e01543. https://doi.org/10.1016/j.heliyon.2019.e01543.
Fu, L., Xu, B.-T., Xu, X.-R., Qin, X.-S., Gan, R.-Y., Li, H.-B., 2010. Antioxidant Capacities and Total Phenolic Contents of 56 Wild Fruits from South China. Molecules 2010, Vol. 15, Pages 8602-8617 15, 8602–8617. https://doi.org/10.3390/MOLECULES15128602.
Gandhi, A.D., Kaviyarasu, K., Supraja, N., Velmurugan, R., Suriyakala, G., Babujanarthanam, R., Zang, Y., Soontarapa, K., Almaary, K.S., Elshikh, M.S., Chen, T.-W., 2021. Annealing dependent synthesis of cyto-compatible nano-silver/calcium hydroxyapatite composite for antimicrobial activities. Arabian J. Chem. 14 (11), 103404. https://doi.org/10.1016/j.arabjc.2021.103404.
Gangwar, M., Gautam, M.K., Sharma, A.K., Tripathi, Y.B., Goel, R.K., Nath, G., 2014. Antioxidant capacity and radical scavenging effect of polyphenol rich Mallotus philippenensis fruit extract on human erythrocytes: an in vitro study. The Scientific World 2014, 1–12. https://doi.org/10.1155/2014/279451.
Grigor'eva, A., Saranina, I., Tikunova, N., Safonov, A., Timoshenko, N., Rebrov, A., Ryabchikova, E., 2013. Fine mechanisms of the interaction of silver nanoparticles with the cells of Salmonella typhimurium and Staphylococcus aureus. Biometals 26 (3), 479–488. https://doi.org/10.1007/s10534-013-9633-3.
Gunaseelan, S., Balupillai, A., Govindasamy, K., Ramasamy, K., Muthusamy, G., Shanmugam, M., Thangaiyan, R., Robert, B.M., Prasad Nagarajan, R., Ponniresan, V.K., Rathinaraj, P., Slominski, A.T., 2017. Linalool prevents oxidative stress activated protein kinases in single UVB-exposed human skin cells. PLoS ONE 12 (5), e0176699.
Guntur, S.R., Kumar, N.S., Hegde, M.M., Dirisala, V.R., 2018. In Vitro Studies of the Antimicrobial and Free-Radical Scavenging Potentials of Silver Nanoparticles Biosynthesized From the Extract of Desmostachya bipinnata. Analytical Chemistry Insights 13. https://doi.org/10.1177/1177390118782877.
Gurunathan, S., Han, J.W., Kwon, D.N., Kim, J.H., 2014. Enhanced antibacterial and anti-biofilm activities of silver nanoparticles against Gram-negative and Gram-positive bacteria. Nanoscale Res. Lett. 9, 1–17. https://doi.org/10.1186/1556-276X-9-373.
Hamouda, R.A., Hussein, M.H., Abo-elmagd, R.A., Bawazir, S.S., 2019. Synthesis and biological characterization of silver nanoparticles derived from the cyanobacterium Oscillatoria limnetica. Sci. Rep. 9 (1). https://doi.org/10.1038/s41598-019-49444-y.
Hemlata, Meena, P.R., Singh, A.P., Tejavath, K.K., 2020. Biosynthesis of Silver Nanoparticles Using Cucumis prophetarum Aqueous Leaf Extract and Their Antibacterial and Antiproliferative Activity against Cancer Cell Lines. ACS Omega 5 (10), 5520–5528. https://doi.org/10.1021/acsomega.0c00155.
Horsten, S., van den Berg, A., Kettenes-van den Bosch, J., Leeflang, B., Labadie, R., 1996. Cyclogossine A: A novel cyclic heptapeptide isolated from the latex of Jatropha gossypifolia. Planta Med. 62 (01), 46–50. https://doi.org/10.1055/s-2006-957795.
Imperio, E., Giancane, G., Valli, L., 2013. Spectral database for postage stamps by means of FT-IR spectroscopy. Anal. chem. 85 (15), 93–7085.
Inbathamizh, L., Ponnu, T.M., Mary, E.J., 2013. In vitro evaluation of antioxidant and anticancer potential of Morinda pubescens synthesized silver nanoparticles. JOPR. J. Pharm. Res. 6 (1), 32–38. https://doi.org/10.1016/j.jopr.2012.11.010.
Kalaimurugan, D., Sivasankar, P., Lavanya, K., Shivakumar, M.S., Venkatesan, S., 2019. Antibacterial and Larvicidal Activity of Fusarium proliferatum (YNS2) Whole Cell Biomass Mediated Copper Nanoparticles. J. Cluster Sci. 30 (4), 1071–1080. https://doi.org/10.1007/s10876-019-01568-x.
Kambale, E.K., Nkanga, C.I., Mutonkole, B.-P., Bapolisi, A.M., Tassa, D.O., Liesse, J.-M., Krause, R.W.M., Memvanga, P.B., 2020. Green synthesis of antimicrobial silver nanoparticles using aqueous leaf extracts from three Congolese plant species (Brillantaisia patula, Crossopteryx febrifuga and Senna siamea). Heliyon 6 (8), e04493. https://doi.org/10.1016/j.heliyon.2020.e04493.
Kang, H.-S., Kim, J.-P., 2019. Butenolide derivatives from the fungus Aspergillus terreus and their radical scavenging activity and protective activity against glutamate-induced excitotoxicity. Appl Biol Chem 62, 43. https://doi.org/10.1186/s13765-019-0451-3.
Kawahara, K., Tsuruda, K., Morishita, M., Uchida, M., 2000. Antibacterial effect of silver-zeolite on oral bacteria under anaerobic conditions. Dent. Mater. 16 (6), 452–455. https://doi.org/10.1016/S0109-5641(00)00050-6.
Mboya, E.A., Sanga, L.A., Ngocho, J.S., 2018. Irrational use of antibiotics in the Moshi Municipality Northern Tanzania: a cross sectional study. PAMJ. 2018; 31:165 31. https://doi.org/10.11604/PAMJ.2018.31.165.15991.
Kiran, M.S., Betageri, V.S., Kumar, C.R.R., Vinay, S.P., Latha, M.S., 2020. In-Vitro Antibacterial, Antioxidant and Cytotoxic Potential of Silver Nanoparticles Synthesized Using Novel Eucalyptus tereticornis Leaves Extract. J. Inorg. Organomet. Polym Mater. 30 (8), 2916–2925. https://doi.org/10.1007/s10904-020-01443-7.
Kolawole, O.S., Jimoh, M.A., Yakubu, F., Chukwuma, E.C., 2017. Taxonomic value of the leaf micro-morphology and quantitative phytochemistry of Jatropha integerrima Jacq. and Jatropha podagrica Hook. (Euphorbiaceae) – known horticultural plants in Nigeria. Anales de Biología (39), 55–62. https://doi.org/10.6018/analesbio.39.06.
Kouhbanani, M.A.J., Beheshtkhoo, N., Taghizadeh, S., Amani, A.M., Alimardani, V., 2019. One-step green synthesis and characterization of iron oxide nanoparticles using aqueous leaf extract of Teucrium polium and their catalytic application in dye degradation. Adv. Nat. Sci.: Nanosci. Nanotechnol. 10 (1), 015007. https://doi.org/10.1088/2043-6254/aafe74.
Krishnaraj, C., Jagan, E.G., Rajasekar, S., Selvakumar, P., Kalaichelvan, P.T., Mohan, N., 2010. Synthesis of silver nanoparticles using Acalypha indica leaf extracts and its antibacterial activity against water borne pathogens. Colloids Surf., B 76 (1), 50–56. https://doi.org/10.1016/j.colsurfb.2009.10.008.
Kuspradini, H., Rosiarto, A.M., Putri, A.S., Kusuma, I.W., 2016. Antioxidant and toxicity properties of anthocyanin extracted from red flower of four tropical shrubs. Nusantara. Bioscience 8 https://doi.org/10.13057/nusbiosci/n080201.

Li, H., Gao, Y., Li, C., Ma, G., Shang, Y., Sun, Y., 2016. A comparative study of the antibacterial mechanisms of silver ion and silver nanoparticles by Fourier transform infrared spectroscopy. Vib. Spectrosc. 85, 112–121. https://doi.org/10.1016/J.VIBSPEC.2016.04.007.

Lobo, V., Patil, A., Phatak, A., Chandra, N., 2010. Free radicals, antioxidants and functional foods: Impact on human health. Pharmacogn. Rev. 4 (8), 118. https://doi.org/10.4103/0973-7847.70902.

Mboya, E.A., Sanga, L.A., Ngocho, J.S., 2018. Irrational use of antibiotics in the Moshi Municipality Northern Tanzania: a cross sectional study. PAMJ. 2018; 31:165 31. https://doi.org/10.11604/PAMJ.2018.31.165.15991.

NilamberLal Das, R., Muruhan, S., Nagarajan, R.P., Balupillai, A., 2019. Naringin prevents ultraviolet-B radiation-induced oxidative damage and inflammation through activation of peroxisome proliferator-activated receptor γ in mouse embryonic fibroblast (NIH-3T3) cells. J. Biochem. Mol. Toxicol. 33 (3), e22263. https://doi.org/10.1002/jbt.2019.33.issue-310.1002/jbt.22263.

Oluwasogo Dada, A., Amoo Adekola, F., Elizabeth Dada, F., Tabitha Adelani-Akande, A., Oluwasesan Bello, M., Rita Okonkwo, C., Abosede Inyinbor, A., Peter Oluyori, A., Olayanju, A., Oluseyi Ajanaku, K., Oluwaseun Adetunji, C., 2019. Silver nanoparticle synthesis by Acalypha wilkesiana extract: phytochemical screening, characterization, influence of operational parameters, and preliminary antibacterial testing. https://doi.org/10.1016/j.heliyon.2019.e02517.

Paosen, S., Saising, J., Septama, A., Piyawan, S., Voravuthikunchaia, S., 2017. Green synthesis of silver nanoparticles using plants from Myrtaceae family and characterization of their antibacterial activity. Mater. Lett. 209, 201–206. https://doi.org/10.1016/j.matlet.2017.07.102.

Plackal Adimuriyil George, B., Kumar, N., Abrahamse, H., Ray, S.S., 2018. Apoptotic efficacy of multifaceted biosynthesized silver nanoparticles on human adenocarcinoma cells. Scientific Reports 2018 8:1 8, 1–14. https://doi.org/10.1038/s41598-018-32480-5.

Pugazhendhi, S., Kirubha, E., Palanisamy, P.K., Gopalakrishnan, R., 2015. Synthesis and characterization of silver nanoparticles from Alpinia calcarata by Green approach and its applications in bactericidal and nonlinear optics. Appl. Surf. Sci. 357, 1801–1808. https://doi.org/10.1016/j.apsusc.2015.09.237.

Rahman, M.M., Islam, M.B., Biswas, M., Khurshid Alam, A.H.M., 2015. In vitro antioxidant and free radical scavenging activity of different parts of Tabebuia pallida growing in Bangladesh. BMC Research Notes 8 (1). https://doi.org/10.1186/s13104-015-1618-6.

Rivero-Montejo, S.d.J., Vargas-Hernandez, M., Torres-Pacheco, I., 2021. Nanoparticles as novel elicitors to improve bioactive compounds in plants. Agriculture (Switzerland) 11 (2), 134. https://doi.org/10.3390/agriculture11020134.

rónavári, andrea, Kovács, D., Igaz, N., Vágvölgyi, csaba, Miklós Boros, I., Kónya, Z., Pfeiffer, I., Kiricsi, M., 2017. Biological activity of green-synthesized silver nanoparticles depends on the applied natural extracts: a comprehensive study. International Journal of Nanomedicine 12–871. https://doi.org/10.2147/IJN.S122842.

Salayová, Aneta, Bedlovičová, Zdenka, Daneu, Nina, Baláž, Matej, Lukáčová Bujňáková, Zdenka, Balážová, Ľudmila, Tkáčiková, Ľudmila, 2021. Green synthesis of silver nanoparticles with antibacterial activity using various medicinal plant extracts: morphology and antibacterial efficacy. Nanomaterials 11 (4), 1005. https://doi.org/10.3390/nano11041005.

Santhoshkumar, J., Sowmya, B., Venkat Kumar, S., Rajeshkumar, S., 2019. Toxicology evaluation and antidermatophytic activity of silver nanoparticles synthesized using leaf extract of Passiflora caerulea. S. Afr. J. Chem. Eng. 29, 17–23. https://doi.org/10.1016/j.sajce.2019.04.001.

Sathiyaraj, Sivaji, Suriyakala, Gunasekaran, Dhanesh Gandhi, Arumugam, Babujanarthanam, Ranganathan, Almaary, Khalid S., Chen, Tse-Wei, Kaviyarasu, K., 2021. Biosynthesis, characterization, and antibacterial activity of gold nanoparticles. J. Infection Public Health 14 (12), 1842–1847. https://doi.org/10.1016/j.jiph.2021.10.007.

Senguttuvan, J., Paulsamy, S., Karthika, K., 2014. Asian Pacific Journal of Tropical Biomedicine journal homepage: www.apjtb.com. Asian Pac J Trop Biomed 4, 359–367. https://doi.org/10.12980/APJTB.4.2014C1030.

Sharma, S.Kr., Singh, H., 2012. A review on pharmacological significance of genus Jatropha (Euphorbiaceae). Chinese Journal of Integrative Medicine 2012 18:11 18, 868–880. https://doi.org/10.1007/S11655-012-1267-8.

Sim, W., Barnard, R.T., Blaskovich, M.A.T., Ziora, Z.M., 2018. antibiotics Antimicrobial Silver in medicinal and consumer applications: a patent review of the past decade (2007–2017). Antibiotics 7, 93. https://doi.org/10.3390/antibiotics7040093.

Skóra, Bartosz, Krajewska, Urszula, Nowak, Anna, Dziedzic, Andrzej, Barylyak, Adriana, Kus-Liśkiewicz, Małgorzata, 2021. Noncytotoxic silver nanoparticles as a new antimicrobial strategy. Sci. Rep. 11 (1). https://doi.org/10.1038/s41598-021-92812-w.

Suriyakala, Gunasekaran, Sathiyaraj, Sivaji, Gandhi, Arumugam Dhanesh, Vadakkan, Kayeen, Mahadeva Rao, U.S., Babujanarthanam, Ranganathan, 2021. Plumeria pudica Jacq. flower extract - mediated silver nanoparticles: characterization and evaluation of biomedical applications. Inorg. Chem. Commun. 126, 108470. https://doi.org/10.1016/j.inoche.2021.108470.

Talapko, Jasminka, Matijević, Tatjana, Juzbašić, Martina, Antolović-Požgain, Arlen, Škrlec, Ivana, 2020. Antibacterial activity of silver and its application in dentistry, cardiology and dermatology. Microorganisms 8 (9), 1400. https://doi.org/10.3390/microorganisms8091400.

Thiel, J., Pakstis, L., Buzby, S., Raffi, M., Ni, C., Pochan, D. J., Shah, S. Ismat, 2007. Antibacterial properties of silver-doped titania. Wiley Online Library 3 (5), 799–803. https://doi.org/10.1002/(ISSN)1613-682910.1002/smll.v3:510.1002/smll.200600481.

Urnukhsaikhan, E., Bold, B.-E., Gunbileg, A., Sukhbaatar, N., Mishig-Ochir, T., 2021. Antibacterial activity and characteristics of silver nanoparticles biosynthesized from Carduus crispus. Sci. Rep. 11, 21047. https://doi.org/10.1038/s41598-021-00520-2.

Wan Mat Khalir, Wan Khaima Azira, Shameli, Kamyar, Jazayeri, Seyed Davoud, Othman, Nor Azizi, Che Jusoh, Nurfatehah Wahyuny, Hassan, Norazian Mohd, 2020. Biosynthesized silver nanoparticles by aqueous stem extract of Entada spiralis and screening of their biomedical activity. Front. Chem. 8. https://doi.org/10.3389/fchem.2020.00620.

Yin, I.X., Zhang, J., Zhao, I.S., Mei, M.L., Li, Q., Chu, C.H., 2020. The Antibacterial Mechanism of Silver Nanoparticles and Its Application in Dentistry . Int. J. Nanomed. 15, 2555–2562. https://doi.org/10.2147/IJN.S246764.

Zahoor, M., Nazir, N., Iftikhar, M., Naz, S., Zekker, I., Burlakovs, J., Uddin, F., Kamran, A.W., Kallistova, A., Pimenov, N., Khan, F.A., 2021. A Review on Silver Nanoparticles: Classification, Various Methods of Synthesis, and Their Potential Roles in Biomedical Applications and Water Treatment. Water 2021, Vol. 13, Page 2216 13, 2216. https://doi.org/10.3390/W13162216.